Denoising of the Uterine EHG by an Undecimated Wavelet Transform

Philippe Carré, Hélène Leman,* Christine Fernandez, and Catherine Marque

***Abstract*— We propose two original methods of denoising of the uterine electrohysterography (EHG) signal by wavelets. This external electrophysiological signal is corrupted by electronic, electromagnetic noises and by the remaining electrocardiogram of the mother. The interfering signals have overlapping spectra. Therefore, a classical filtering is unusable. Wavelets should be a very well-suited denoising tool.**

The first proposed method uses the algorithm "à trou" with nonsymmetrical filters. The computation is rapid and the results are satisfying compared to the classical denoising techniques.

The second algorithm is an improvement of the first method. It uses orthogonal wavelets and the result of the thresholding corresponds to the average of all circulant shifts denoised by a decimated wavelet transform.

Results are compared to traditional denoising algorithms by wavelet (orthogonal, maximally decimated). The proposed algorithms are more efficient on simulated signals as well as on uterine EHG.

***Index Terms*— Correlated noise, noise reduction, uncorrelated noise, undecimated wavelet transform, uterine EHG, wavelet shrinkage.**

I. Introduction

ABDOMINAL uterine electrohysterography (EHG) is a recently used technique for the recording of uterine contractions during women's pregnancy. A few studies have already proved that the EHG signal is able to provide reliable information about uterine contractions [1]–[6]. The improvements in biological signal recordings and processing methods will allow this signal to be used for the early detection of preterm deliveries [7]. We thus plan to monitor the contractions of women at high risk of preterm delivery by means of noninvasive EHG recording.

The EHG is an external signal of very low amplitude (below 1 mV), whose main energy is ranging from 0.2 to 4 Hz. In spite of the analogical filtering during acquisition, it is noised by many other signals (remaining of electrocardiogram, electromagnetic noise, ...). To remove these noises from the signal, it is impossible to use classical filtering because the frequencies of the noise are in the same frequency bands as those of the signal. Consequently, due to its ability to split signal and noise, the wavelet theory is very well suited to EHG denoising.

In this paper, we propose two new methods for denoising the uterine EHG, using an undecimated wavelet transform (the algorithm "à trous" [8]). The first method uses nonsymmetrical filters inspired by Bijaoui's algorithm proposed for spatial images [9], [10]. The second one is an improvement of the first method and uses quadrature mirror filters.

Manuscript received April 2, 1997; revised March 27, 1998. This work was supported in part by the "Pôle régional GBM Périnatalité" of the Picardie region and by the CNRS. *Asterisk indicates corresponding author.*

P. Carré and C. Fernandez are with the Ircom-SIC Laboratory, UMR CNRS 6615, 86960 Futuroscope, France.

*H. Leman is with the Department of Biomedical Engineering, UMR CNRS 6600, Compiègne University of Technology (UTC), Compiègne Cedex, France (e-mail: helene.leman@utc.fr).

C. Marque is with the Department of Biomedical Engineering, UMR CNRS 6600, Compiègne University of Technology (UTC), Compiègne Cedex, France.

Publisher Item Identifier S 0018-9294(98)05895-9.

II. Electrohysterography

The usual obstetrical practice includes uterine activity monitoring by two different means [11]. An external mechanical recording method, referred to as external tocography, allows the measurement of the abdominal wall deformations due to the effect of uterine contractions. It measures only the rate of appearance of contractions and is very sensitive to the abdominal wall motions. An internal recording method allows the measurement of intrauterine pressure by means of an intrauterine catheter. But detailed uterine activity evaluation is not possible by means of this global measurement. Furthermore, catheter positioning is an invasive act that requires a strict aseptic state and cannot be considered as a routine procedure for pregnancy monitoring.

As for striated muscle, the uterine mechanical contraction is due to an electrical command, the electromyographic activity of uterine smooth cells. The electrical activity, picked up on the abdominal wall, represents the summation of electrical activities of the uterine cells underlying the electrodes. The EHG, thus, represents this electrical command of the contraction [Fig. 2(A)] [12]. This signal also contains information related to foetal movements which are represented by spikes superimposed on the baseline. As the trigger of the contraction, it should be much more representative of the physiology of uterine activity than the tocography and, therefore, would provide an attractive way of monitoring uterine activity.

The EHG is picked up by means of one electrode pair. The Ag-AgCl Beckman electrodes (8 mm in diameter, 25-mm spaced centers) are positioned on the abdominal wall after careful preparation of the skin, which lowers the interelectrode impedance of about 10 kΩ.

The electrode pair is set over the umbilicus, lined up with the median vertical axis of the uterus. The ground electrode is located on the woman's hip.

The EHG signal is differentially amplified, bandpass filtered (0.2–8 Hz), amplified and sampled (sample rate 16 Hz).

The obtained signal is not stationary. The filter-bank and wavelet decomposition theory are, thus, very well-suited for the analysis of this signal.

III. Denoising by Wavelet Transform

A. The Wavelet Transform

The discrete wavelet transform (DWT) stems from the multiresolution analysis and filter bank theory [13]. The multiresolution analysis is a decreasing sequence of closed subspace $\{V_j\}_{j\in Z}$ which approximate $L^2(\Re)$. A function $f(x)\in L^2(\Re)$ is projected, at each step j, onto the subset V_j. This projection is defined as the scalar product, noted s_j, of $f(x)$ with a scaling function, noted $\phi(x)$

$$s_{j,k}\triangleq\left\langle f(x),2^{-j}\phi\left(2^{-j}x-k\right)\right\rangle. \tag{1}$$

k is the translation parameter and j is the dilatation parameter. $\phi(x)$ has the following property:

$$\frac{1}{2}\phi\left(\frac{x}{2}\right)=\sum_n h(n)\phi(x-n). \tag{2}$$

The sequence $\{h(k),k\in Z\}\in l^2$ is the impulse response of a low-pass filter.

At each step, the signal is smoothed. The lost information can be restored using the complementary subspace W_{j+1} of V_{j+1} in V_j. This subspace is generated by a wavelet $\psi(x)$ with integer translation and dyadic dilatation; the projection of $f(x)$ on W_j is defined as

$$d_{j,k}\triangleq\left\langle f(x),2^{-j}\psi\left(2^{-j}x-k\right)\right\rangle. \tag{3}$$

The sequence $\{g(k),k\in Z\}\in l^2$ is the impulse response of a high-pass filter. As the scaling function, the wavelet function has the following property:

$$\frac{1}{2}\psi\left(\frac{x}{2}\right)=\sum_n g(n)\phi(x-n). \tag{4}$$

Then, the analysis is defined as

$$\begin{aligned}s_{j,k}&=\tfrac{1}{2}\sum_n h(n-2k)s_{j-1,k}\\ d_{j,k}&=\tfrac{1}{2}\sum_n g(n-2k)s_{j-1,k}.\end{aligned} \tag{5}$$

For orthogonal wavelets, the restoration is performed with

$$s_{j,k}=2\sum_n h(k-2n)s_{j+1,n}+2\sum_n g(k-2n)d_{j+1,n}. \tag{6}$$

Mallat's multiresolution analysis is connected with so called "pyramidal" algorithms in image processing [14]. The filters $h(k)$ and $g(k)$ are quadrature mirror filters.

In order to get an exact restoration, two conditions are required on the conjugate filters (in the biorthogonal case) [15]

$$H(\xi)\tilde{H}^*(\xi)+G(\xi)\tilde{G}^*(\xi)=1 \tag{7}$$

which implies a correct data restoration of one scale to the other, and

$$H(\xi+\pi/2)\tilde{H}^*(\xi)+G(\xi+\pi/2)\tilde{G}^*(\xi)=0 \tag{8}$$

which represents the compensation of recovery effects introduced by the downsampling.

Because of decimation, the Mallat's decomposition is completely time variant. A way to obtain a time-invariant system is to compute all the integer shifts of the signal. At scale i, the z-transform of the equivalent filter is [16]

$$G_i(z)=G(z^{2^{i-1}})\prod_{k=0}^{i-2}H(z^{2^k}). \tag{9}$$

This algorithm was named algorithm "à trous" [8]. Its link with the Mallat's algorithm is discussed in [17]. Because the decomposition is not decimated, filters are dilated between each projection. Therefore, each wavelet's scale has N points. For the scale i, these N points correspond to 2^i different decompositions obtained with the decimated transform using all the circulant shifts of the signal. These decompositions, each one composed of $N/2^i$ points, are intertwined.

The algorithm "à trous" presents many advantages.

- *A simpler filter selection*. Condition (8), which was required for a perfect reconstruction, is no more necessary because coefficients are no longer downsampled.
- *A knowledge of all wavelets' coefficients.* Coefficients removed during the downsampling are not necessary for a perfect reconstruction, but they may contain information useful for the denoising.
- *An intertwining of orthogonal decompositions.* The decomposition is not orthogonal because of the information redundancy, but if the used filters are associated to an orthogonal basis, the algorithm "à trous" keeps all the orthogonal decompositions.

In this work, we propose two denoising algorithms using the decomposition "à trous."

B. Denoising

1) White Noise: In the case of an additive white Gaussian noise, the problem consists in determining the real signal, noted $f(t)$, when we just know the measurements x_i defined as

$$x_i=f(t_i)+\sigma b_i,\ \text{with } i=0\cdots N,\ b_i\overset{\text{i.i.d}}{\sim}N(0,1),\ \text{and } \sigma>0. \tag{10}$$

If the basis of wavelets is orthogonal, the white noise remains a white noise of the same magnitude. Moreover, this noise is completely uncorrelated in all the scales. Consequently, we can rewrite (10) as

$$Wx_i=Wf(t_i)+\sigma d_i^b,\ \text{with } d_i^b\overset{\text{i.i.d}}{\sim}N(0,1). \tag{11}$$

d_i^b denotes the decimated orthogonal wavelet transform of the noise and W is the wavelet transform.

In order to reconstruct the function $f(t)$ from measures x_i, we just have to remove the noise contribution from each Wx_i. The level of noise is unknown. But it can be estimated by a value, noted λ. Donoho and Johnstone have proposed two types of shrinkage functions [noted $T_\lambda(\cdot)$] [18].

- "Soft thresholding," defined as

$$T_\lambda^{\text{Soft}}(d_{j,k})=\operatorname{sgn}(d_{j,k})\left(|d_{j,k}|-\lambda\right)_+. \tag{12}$$

- "Hard thresholding," defined as

$$T_\lambda^{\text{Hard}}(d_{j,k})=d_{j,k}\cdot 1_{[|d_{j,k}|\geq\lambda]}. \tag{13}$$

A variety of methods have been proposed for the estimation of λ [19], [9]. The first one is the Donoho and Johnsone's *VisuShrink* universal threshold; λ is defined as [20]

$$\lambda = \sigma\sqrt{2\log(n)}, \quad \text{with} \quad \sigma = \text{MAD}/0.6745 \tag{14}$$

and n the number of data samples.

MAD is the median absolute value estimated on the coefficients of the finest scale. The factor 0.6745 is chosen after a calibration with a Gaussian distribution. The noise dispersion is estimated on the first scale which mainly contains noise coefficients.

2) Correlated Noise: In the literature, most of denoising methods only study the case of a white Gaussian noise. Johnstone and Silverman [21] have studied the case of a correlated noise, allowing, thus, the formalization of practical method. The main properties of the wavelet decomposition of a stationary correlated noise are the following.

- The correlation of coefficients in same scale decreases very fast as soon as we tend to the coarsest scales.
- The correlation of coefficients between two different scales is very small, or null. This results comes from the use of bandpass filters during the coefficient computations.

The log-variance of the noise decreases roughly linearly with the scale. On each scale, the noise coefficients follow approximately a Gaussian distribution [21]. From these statements, Johnstone and Silverman propose a new denoising method using a level-dependent thresholding

$$\lambda_i = \sigma_i\sqrt{2\log(n_i)}, \quad \text{with}$$
$$\sigma_i = \text{MAD}_i/0.6745 \text{ and } i \text{ the scale.} \tag{15}$$

3) Notations: We will use the shrinkage function $T_\lambda(\cdot)$ defined as (12) or (13).

We define P and Q projection operators of V_j on V_{j+1} and W_{j+1}, respectively. We will note $P_\perp$ and $Q_\perp$ the projection operator for the decimated case and P_u and Q_u for the undecimated case. Opposite operators are noted $P_\perp^{-1}$, $Q_\perp^{-1}$, P_u^{-1}, and Q_u^{-1}.

For the ith scale, we note w_i, the undecimated wavelet coefficients, and c_i, undecimated low-pass approximation of the signal. d_i is the decimated wavelet coefficients, and s_i, the decimated low-pass approximation of the signal.

With the previous notations, the undecimated and decimated wavelet transformations are defined as

$$w_i = Q_u(c_{i-1}) \quad \text{and} \quad c_i = P_u(c_{i-1})$$
for the undecimated wavelet transform
$$d_i = Q_\perp(s_{i-1}) \quad \text{and} \quad s_i = P_\perp(s_{i-1})$$
for the decimated wavelet transform.

IV. Denoising of Uterine EHG by the Algorithm "`a trous" with Nonsymmetrical Filters

This method is based on Bijaoui's papers [9], [10], dealing with the denoising of the spatial images. They use very simple methods for complex problems. We propose some modifications to these algorithms for signals corrupted by correlated noise. We apply this method for the EHG denoising.

A. Principles

1) Decomposition and Reconstruction: For a perfect reconstruction, the algorithm "à trous" requires that the filters verify (7).

Bijaoui's idea [9] is to define the high-pass filter, $G(\xi)$ as

$$G(\xi) = 1 - H(\xi) \text{ with } H(\xi) \text{ the low-pass filter} \tag{16}$$

and the reconstruction filters are defined as

$$\tilde{H}(\xi) = \tilde{G}(\xi) = 1. \tag{17}$$

It is easy to verify that filters defined in (16) and (17) satisfy (7) for all $H(\xi)$.

From (16), wavelet coefficients are simply computed by the difference between two successive smoothed sequences

$$w_{j+1,k} = c_{j+1,k} - c_{j,k} \tag{18}$$

and the reconstruction is the sum of all wavelet scales, plus the smoothed signal at the coarsest scale

$$c_{0,k} = \sum_{i=1}^{L} w_{i,k} + c_{L,k}$$
with L number of decomposition scales. (19)

The scaling function is the B_3-Spline, and the associated filter $H(\xi)$ is [14]

$$H(z) = \tfrac{1}{16}z^{-2} + \tfrac{1}{4}z^{-1} + \tfrac{3}{8} + \tfrac{1}{4}z + \tfrac{1}{16}z^2. \tag{20}$$

The filter associated to the wavelet is [9]

$$G(z) = -\tfrac{1}{16}z^{-2} - \tfrac{1}{4}z^{-1} + \tfrac{5}{8} - \tfrac{1}{4}z - \tfrac{1}{16}z^2. \tag{21}$$

The limit of this definition is that filters are not quadrature mirror filters. The consequence is a nonorthogonal decomposition, with a correlation between scales. The frequencies, close to the cutoff high-pass frequency, will be also repeated on the following scale.

2) Denoising: We have already seen that the orthogonal decomposition presents some qualities for denoising.

- A white noise remains a white noise in an orthogonal decomposition.
- The noise spreads in scales in the form of small coefficients.
- The signal is represented by larger coefficients.

In a nonorthogonal decomposition, the first property is not true because of the correlation existing between coefficients of the different scales. On the other hand, we have observed that the two other properties remain true. Since this decomposition allows a perfect reconstruction, it has, therefore, the property to keep the structure of the signal: the energy of the noise does not concentrate on some coefficients, contrary to the signal; and the energy of noise is smaller than the energy of signal.

Thus, even with nonorthogonal decomposition, coefficients from noise correspond to weak coefficients and signal to larger ones. Therefore, the proposed denoising method uses the same principle as the orthogonal downsampling decomposition [(11)]: to apply a thresholding on wavelet coefficients, so as to remove the smaller coefficients.

In order to estimate the threshold, it is necessary to study the coefficient distribution. In the nonorthogonal case, it is difficult to conceive a mathematical model. Nevertheless, we can make two remarks about the numerical results we obtained.

- Noise coefficients are distributed around zero. Indeed, if the noise is stationary, we have

$$E(w_{i,k}^B) = E\left[\sum_n c_{i-1,k+2^i n}^B g(n)\right] = \overline{c}_{i-1}^B \sum_n g(n) = 0 \tag{22}$$

  $w_{i,k}^B$ and $c_{i-1,k}^B$ the noise coefficients, and $\overline{c}_{i-1}^B = E(c_{i-1}^B)$.
- Noise coefficients follow approximately a Gaussian distribution. Indeed, after filtering, the obtained signal can be considered as a realization of a sum of infinitesimal independent random variables, which allows the application of the central limit theorem.

Then, in order to solve the denoising problem, we applied the theory of decision: $w_{i,k}$ are compared to $\alpha_i \sigma_i$ where σ_i is the noise standard deviation in ith scale, and $\alpha_i \in \Re^{+*}$. The statistical estimation methods of the noise level presented for orthogonal decomposition, cannot be applied to a nonorthogonal decomposition. For this case, and with a white noise, Bijaoui has proposed another estimation technique, which is based on the decomposition of a simulated Gaussian field [9], [10]. For our application, we have chosen a simpler strategy, often applied to image segmentation. We simply evaluated the noise level from the estimation of the standard deviation of the wavelet coefficients for each scale. Indeed, even for the white noise, the noise level is not constant on all the scales in a nonorthogonal decomposition. The thresholding is, therefore, defined as

$$T(w_{i,k}) = w_{i,k} \cdot 1_{[|w_{i,k}| \geq \alpha_i \sigma_i]}, \quad \text{with}$$
$$\sigma_i = \sqrt{\frac{1}{N+1} \sum_{k=0}^{N} (w_{i,k})^2}. \tag{23}$$

We use the hard thresholding that is optimum for the l_2 reconstruction error. In the case of the decimated decomposition, this thresholding exhibits parasitic oscillations. Because of the information redundancy, our algorithm solves this problem.

Coefficients α_i are defined according to the application. For the uterine EHG, we use a value of three, which induces the suppression of 99.8% of coefficients in a Gaussian distribution.

B. Results

The above described algorithm, has been implemented in Matlab. We apply this algorithm on test signal (*Blocks* [18], [20], and [22]), corrupted by a correlated noise. Fig. 1 presents the results of denoising, by Johnstone–Silverman method with Daubechies wavelet D4 [23], and by the proposed algorithm.

We can see that the noise is efficiently removed by our algorithm, and that the signal presents fewer distorsions than Johnstone's result, especially at the discontinuities.

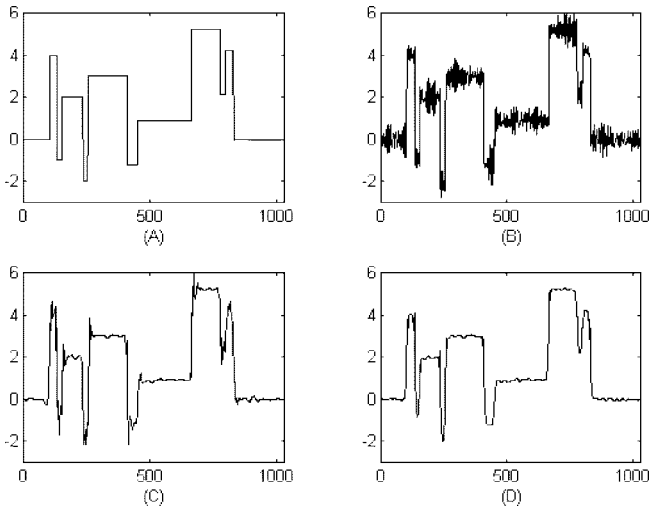

Fig. 1. Denoising of Blocks corrupted by a correlated noise: (A) blocks signal (B) blocks noised SNR = 6, (C) denoising by Johnstone–Silverman method, and (D) denoising by our algorithm.

We then applied this method on 120 contractions for a study on the early detection of preterm delivery [7]. For the denoising, we have decomposed the signal in three wavelet scales.

The result of this method is shown in Fig. 2. We can notice that the baseline amplitude is reduced, while conserving the other events of interest: spikes related to foetal movements. The burst of activity related to the uterine contraction is preserved.

To evaluate the quality of this method, we have applied on this signal, "classical" denoising techniques by wavelets. We made no hypothesis on the nature of the noise and, thus, applied Donoho's algorithm, conceived for white noise, and Johnstone's algorithm, conceived for correlated noise. These two algorithms are used with Daubechies wavelets D_4 [23]. For a better visual comparison, Fig. 3 shows the results of these methods on a zoom of the signal. We can first observe that the thresholding by Johnstone's technique gives better results than Donoho's algorithm. Indeed, the reconstructed signal by Donoho's method is much more irregular and seems, thus, noisier. We deduce that the noise corrupting the EHG does not follow a Gaussian model and, therefore, an evaluation of the threshold on each wavelet scale is more appropriate.

The signal denoised by our method is smoother and the rejection of the noise seems to be more effective.

C. Remarks

The algorithm advantages are that it is simple to implement and rapid. A first study of the EHG characteristics has been made after denoising by the nonorthogonal method and has given many interesting results [7]. The rapidity of this algorithm would make it very attractive for a real-time processing. Indeed, hardware implementation could be easily conceived for a portable electronic case.

Nevertheless, the simple definition of analysis and reconstruction filters limits its results.

- Reconstruction filters, defined in (17), are all-pass. The suppression of a coefficient, by hard thresholding, may

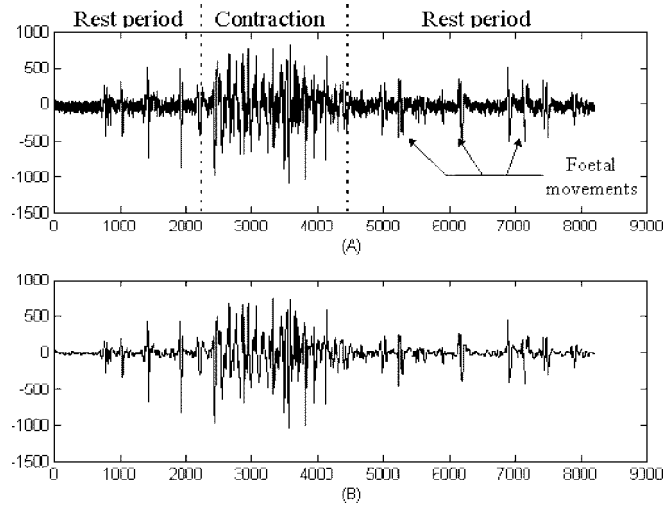

Fig. 2. Denoising of EHG signal by nonorthogonal method. (A) Original signal and (B) denoised signal.

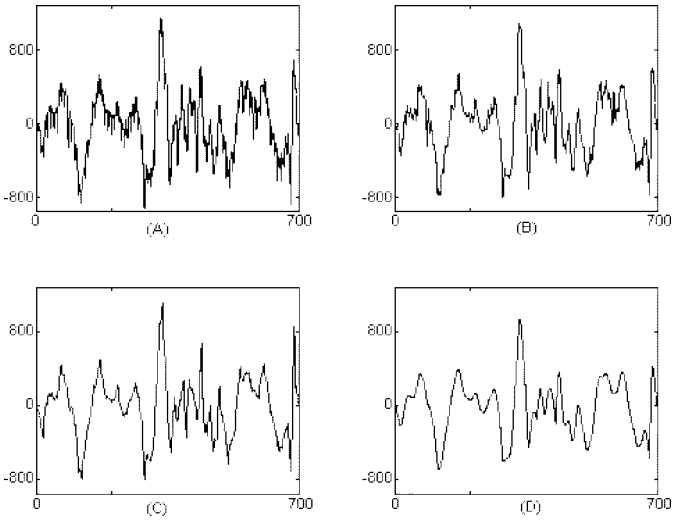

Fig. 3. Zoom of the uterine EHG. (A) Original signal, (B) denoising by Donoho's algorithm, (C) denoising by Johnstone's algorithm, and (D) denoising by our method.

create artificial frequencies. A reconstruction with band-pass filters removes these parasitic frequencies. This is not the case with $\tilde{H}(\xi) = \tilde{G}(\xi) = 1$, inducing some artificial peak appearance.

- Analysis filters are not quadrature mirror filters. The statistical study of a nonorthogonal decomposition is complex, so the threshold can be fixed only with an empirical method.

We propose an improvement of this method, which uses quadrature mirror filters, while preserving the principle of the undecimated decomposition.

V. EHG Denoising by the Algorithm "À trous" with Orthogonal Wavelets

A. Principles of the Algorithm

With the algorithm "à trous", it is possible to obtain all intertwined decimated decompositions. Because of the information redundancy, the decomposition is not orthogonal and wavelet coefficients of the same scale are correlated. But if the filters are associated by an orthogonal base, then the correlation between the coefficients is simply due to the information redundancy. In this case, all intertwined decimated transforms are orthogonal (if we study them separately). Due to the "orthogonal" filters, the different scales are independent.

The new proposed algorithm, which is called *uwt_mean*, is based on this principle. Let us demonstrate the qualities of this algorithm.

1) Undecimated Wavelet Coefficient Thresholding: We will prove that the result of the thresholding of the wavelet coefficient matrix obtained without downsampling defined as $T_\lambda([w_1|w_2|\cdots|w_{L-1}|w_L])$, with λ, a threshold to be defined, corresponds to the average of all circulant shifts denoised by a decimated wavelet transform (with the algorithm of Donoho–Jonhstone).

Decomposition and thresholding: For the scale i, undecimated wavelet coefficients, noted w_i, can be written as

$$w_i = \left\{d_i^{0/i-1}\right\} \ \vec{\cup} \ \left\{d_i^{1/i-1}\right\} \tag{24}$$

with $\vec{\cup}$ a combination with intertwining of coefficients, and $d_j^{k/i}$ is the "pseudo-decimated" wavelet coefficients obtained, at the jth scale, with the decimated wavelet transform of the k-shifted undecimated low-pass approximation of the signal at the ith scale

$$d_j^{k/i} = Q_\perp (P_\perp)^{j-i-1}\big(TR_k(c_i)\big) \tag{25}$$

with $Q_\perp(P_\perp)^{j-i-1}[f] = Q_\perp \circ P_\perp \circ \cdots P_\perp[f]$ and TR_k shift operator defined by

$$TR_k\big(f(t)\big)\,(t) = f(t-k).$$

We can notice that $d_i = d_i^{0/0}$.

Proposition 1: If w_i are the undecimated wavelet coefficients for the scale i, they can be written as

$$w_i = \overrightarrow{\bigcup_{k=0\cdots 2^i-1}} d_i^{k/0}.$$

The proof is done in Appendix I.

If a thresholding $T_\lambda(\cdot)$ is applied to undecimated wavelet coefficients w_i, then

$$T_{\lambda_i}(w_i) = T_{\lambda_i}\left(\overrightarrow{\bigcup_{k=0\cdots 2^i-1}} d_i^{k/0}\right). \tag{26}$$

We can define, for each sequence $d_i^{k/0}$, a threshold, noted λ_i^k. In this case, (26) can be written

$$T_{\lambda_i}(w_i) = \overrightarrow{\bigcup_{k=0\cdots 2^i-1}} T_{\lambda_i^k}\left(d_i^{k/0}\right). \tag{27}$$

From (25), we can see that each set $\{d_1^{k/0}|d_2^{k/0}\cdots|d_L^{k/0}\}$ corresponds to an orthogonal decomposition and can be studied independently. So, the thresholding defined by Johnstone for correlated noise can be applied on each subset $d_i^{k/0}$ with

$$\lambda_i^k = \sigma_i^k \sqrt{2\log\left(N_i^k\right)} \tag{28}$$

with N_i^k, the number of coefficients in the subset $d_i^{k/0}$. This number is defined as

$$N_i^k = \frac{N}{2^i} \tag{29}$$

and the noise level is estimated by

$$\sigma_i^k = \mathrm{MAD}\left(d_i^{k/0}\right)/0.6745. \tag{30}$$

In our numerical examples, we have noticed that the estimated value of the noise level remain approximately constant for the different subsets of a same scale, because of information redundancy. For a limited number of scales (i.e., all N_i^k are large enough)

$$\begin{aligned}\mathrm{MAD}\left(d_i^{0/0}\right) \simeq \mathrm{MAD}\left(d_i^{1/0}\right) \simeq \cdots \mathrm{MAD}\left(d_i^{2^i-1/0}\right)\\ \Longrightarrow \sigma_i^0 \simeq \sigma_i^1 \simeq \sigma_i^2 \cdots \simeq \sigma_i^{2^i-1}\end{aligned} \tag{31}$$

then

$$\mathrm{MAD}(w_i) \simeq \mathrm{MAD}\left(d_i^{0/0}\right) \simeq \cdots \mathrm{MAD}\left(d_i^{2^i-1/0}\right). \tag{32}$$

Moreover, we can notice that the number of coefficients in subsets, N_i^k, are constant for a scale i, and are equal to $N/2^i$. Then, all local thresholds are equal

$$\lambda_i^0 \simeq \lambda_i^1 \cdots \simeq \lambda_i^{2^i-1}.$$

We can, therefore, define a thresholding with, for a scale i, a global threshold λ_i

$$\lambda_i = \sqrt{2\log(N/2^i)} * \mathrm{MAD}(w_i)/0.6745 \tag{33}$$

2) Forward Transform:

Proposition 2: If $\tilde{f}$ is a function obtained after inverse transformation of thresholded undecimated wavelet coefficients and $\tilde{f}_b$ corresponds to the inverse transform obtained after denoising with the algorithm of Donoho–Johnstone on the shift function $TR_b(f)$, then

$$\tilde{f} = \frac{1}{2^L}\left[\tilde{f}_0 + \tilde{f}_1 + \cdots + \tilde{f}_b + \cdots + \tilde{f}_{2^L-1}\right]$$

with L the number of scales.

The proof is shown in Appendix II.

This proposition shows that the application of a thresholding on an undecimated wavelet transform, with a threshold defined by (33), is equal to the average of all circulant shifts denoised by a decimated orthogonal wavelet transform.

Each function $\tilde{f}_b$ has two *theoretical* properties [18].

- The noise has been almost entirely suppressed.
- Features sharp in the original remain sharp in reconstruction.

Since the function $\tilde{f}$ is the result of the average of all $\tilde{f}_b$, obtained by our *uwt_mean* algorithm, it has the same properties. Moreover, the average reduces artifacts which appear after thresholding of the traditional orthogonal wavelet transform. Because of the information redundancy, the algorithm can use the hard thresholding, that optimizes the l^2 reconstruction error.

3) Remarks: We have proposed the *uwt_mean* algorithm in the general case of a correlated noise. But the same method can be used for a white noise, with a threshold estimated on the first scale and applied on the following. We can also define the *uwt_mean* algorithm with a soft thresholding.

A similar approach, called "translation-invariant denoising," has been proposed recently by Coifman and Donoho [22].

The main difference between our *uwt_mean* algorithm and "TI denoising" is the definition of the threshold: the "translation-invariant denoising" method applies a constant threshold for all scale ($\sqrt{2\log(N)}$ is the same for all scales). Our threshold decreases with scales ($\sqrt{2\log(N/2^i)}$ is not constant), because we consider that the undecimated ith scale has $N/2^i$ coefficients "repeating" 2^i times.

With small oscillations, the l^2 reconstruction error of *uwt_mean* is better than "translation-invariant" [24] because the constant "TI denoising" threshold is too large for rough scales. Then, coefficients which correspond to small oscillations are killed. We can notice that Coifman and Donoho have not proposed a method in order to estimate the noise level σ with an undecimated wavelet transform. In their paper, they use test signals corrupted by an additive white noise with a variance equal to one.

B. Results of the uwt_mean Algorithm

The algorithm *uwt_mean*, for correlated and white noise, has been implemented in C and Matlab. We have tested it on the synthetic signals used in Donoho–Johnstone's papers. On a second step, the *uwt_mean* algorithm has been applied to EHG.

1) Results of the uwt_mean Algorithm on Test Signals: The denoising algorithms are implemented with Daubechies wavelets D_4, with four vanishing moments [23]. Fig. 4 shows the case of the addition of a white noise on *Block*s signal, with variance equal to one. The *uwt_mean* algorithm gives better results than VisuShrink method: the reconstructed signal is smoother. On VisuShrink's result, the parasitic oscillations, called by Coifman and Donoho "pseudo-Gibbs" [22], are especially present at discontinuities. It is obvious that these pseudo-Gibbs are mostly reduced by the *uwt_mean* algorithm.

If the wavelets are not regular (for example the Haar wavelets) the efficiency of the *uwt_mean* algorithm is even more noticeable. The VisuShrink's method with Haar wavelets presents another kind of artifact: the stairstep nature of the partial Haar approximations in regions of smooth behavior (Fig. 5 with *Doppler* signal noised by a white Gaussian noise). We can see that the *uwt_mean* reconstruction demonstrates no stairstep character.

The same results have been obtained with correlated noise [24].

2) Results of the uwt_mean Algorithm on the Uterine EHG Signal: We have then applied the *uwt_mean* algorithm on the uterine EHG signal with a level-dependent threshold (correlated noise). The signal has been decomposed in three wavelet scales. Fig. 6 shows the result of *uwt_mean* denoising: the noise is removed (smaller baseline) and the oscillations of the contraction are kept.

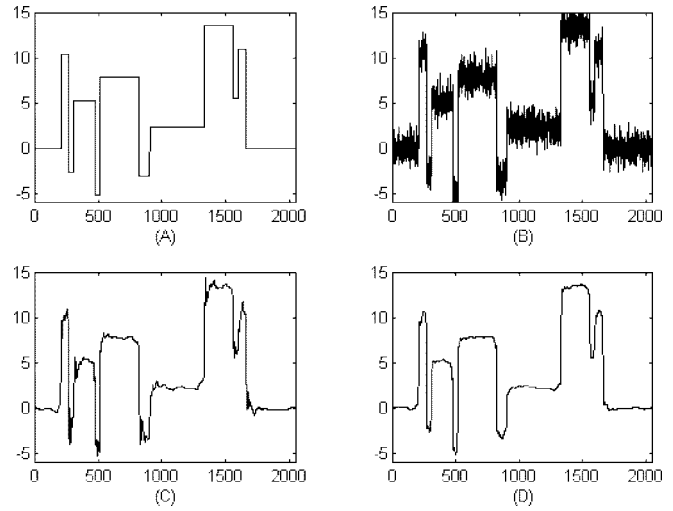

Fig. 4. Denoising of Blocks noised by a Gaussian white noise: (A) blocks, (B) blocks noised SNR = 5, (C) denoising by VisuShrink, and (D) denoising by *uwt_mean*.

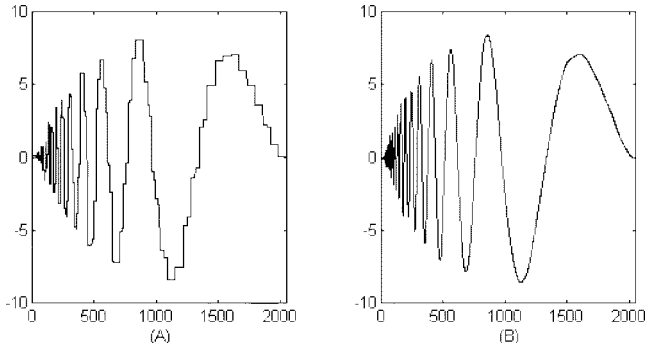

Fig. 5. Denoising of Doppler with Haar wavelets: (A) VisuShrink and (B) *uwt_mean*.

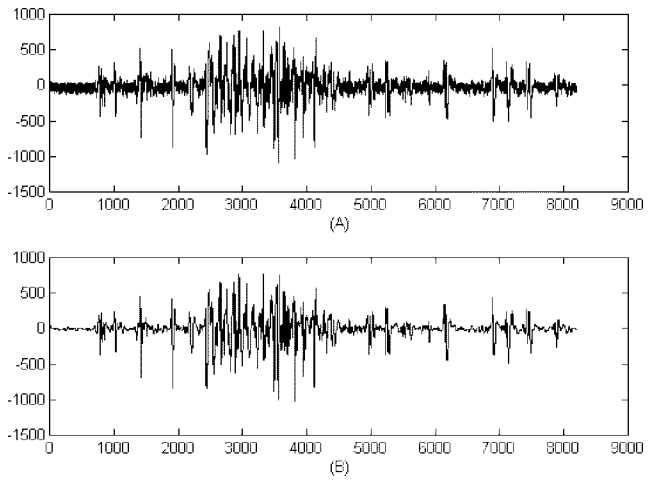

Fig. 6. Denoising of EHG signal by *uwt_mean:* (A) original signal and (B) denoised signal.

This better denoised baseline makes the detection of the onset of the contraction easier. This leads to easier automatic segmentation of the contractions.

In order to study the differences between all these algorithms, a close-up of the signal is shown in Fig. 7. Johnstone's reconstruction keeps the global shape of the contraction, but removes some small oscillations. Moreover, we can see that the obtained signal is irregular since the forms of the oscillations are triangular and sharp. The nonorthogonal method keeps more small oscillations, but the smallest are reconstructed with the same suspicious artefactual peaks as those obtained after denoising of the *Doppler* test signal, corrupted by a correlated noise [Fig. 8(A)]. On both signals [Figs. 7(D) and 8(B)], the *uwt_mean* algorithm follows precisely the shape of the signal, keeps all oscillations and removes efficiently the noise.

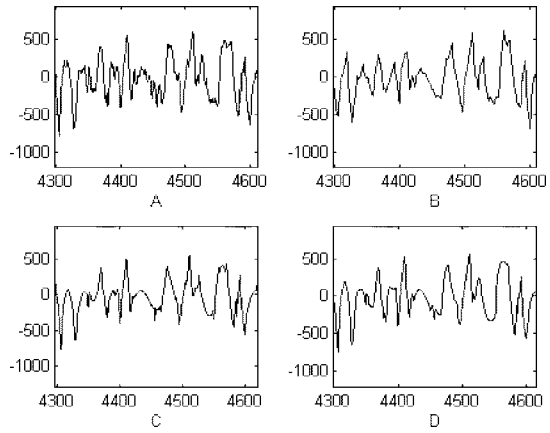

Fig. 7. Zoom of the uterine EHG signal: (A) original signal, (B) denoising by Johnstone's method, (C) denoising by the nonorthogonal wavelet method, and (D) denoising by the *uwt_mean* algorithm.

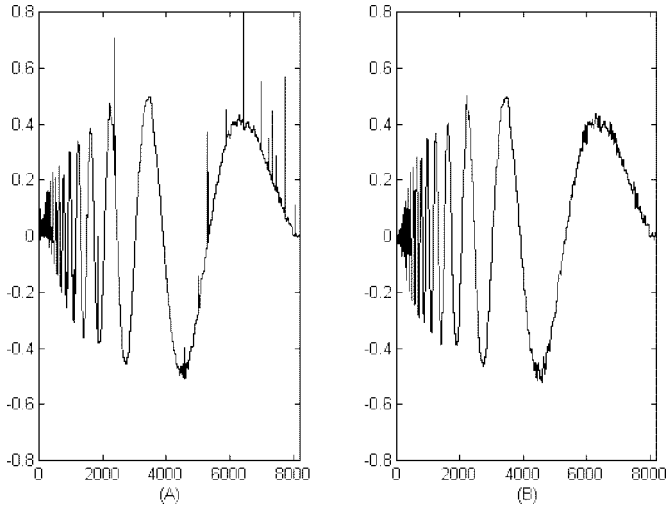

Fig. 8. Denoising of Doppler corrupted by an additive noise: (A) nonorthogonal method and (B) *uwt_mean*.

C. Influence of the Denoising on the Instantaneous Frequency of the Signal

The instantaneous frequency, estimated by the method of the analytic signal [25] is a parameter used in a preliminary study for the early detection of preterm delivery [7]. This curve is continuous and represents the time evolution of the mean frequency. Let us demonstrate the importance of denoising on this estimated instantaneous frequency of uterine EHG.

We compare the estimated instantaneous frequency of the contraction and of a short part of the baseline [Fig. 9(B)–(D)]. The first thing to notice is that the instantaneous frequency

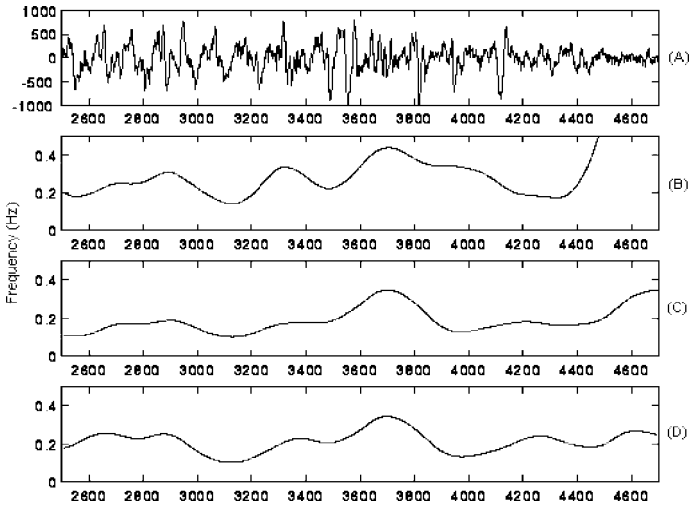

Fig. 9. (A) Zoom of original signal, (B) instantaneous frequency of original signal, (C) signal denoised by nonorthogonal method, and (D) signal denoised by *uwt_mean*.

evolution computed from the two denoised signals have similar behavior for the contraction. On the other hand, the behavior of the instantaneous frequency of the noised signal is different. The instantaneous frequency of the denoised baseline is considerably reduced, compared to the values computed on the original signal (over 0,5 Hz). This demonstrates the efficiency of denoising. Since noise is composed of higher frequencies than the signal, the instantaneous frequency of the noised baseline increases. After denoising, the baseline mainly contains normal small oscillations which are related to the relaxed uterus state.

Therefore, denoising greatly influences the estimated instantaneous frequency of the signal. In the presence of noise, the instantaneous frequency exhibits aberrant high values. After denoising, the values are lower and closer to the real values presented in the literature [26].

A proper denoising is, thus, very important for the analysis of the EHG signal.

VI. Conclusion

In this study, we presented two original methods of denoising using the algorithm "à trous" which possesses many advantages: the choice of very simple filters, and the nondecimation of the coefficients.

The first method, based on nonorthogonal transform, was first proposed by Bijaoui. It is rapid and easy to implement. The results are good but the algorithm creates some artefactual peaks which affect the signal.

The second method uses orthogonal wavelets and gives very good results on simulated signals as well as on the EHG signal because of its intrinsic averaging. Small oscillations of the contractions are kept without parasitic peaks and noise is efficiently removed from the signal, giving a quiet baseline between contractions.

Among the studied methods, *uwt_mean* seems, thus, to be the most adapted for the denoising of the uterine EHG signal.

Appendix I

If w_i are the undecimated wavelets coefficients for the scale i, they can be written as

$$w_i = \overrightarrow{\bigcup_{k=0\cdots 2^i-1}} d_i^{k/0}.$$

Proof: For the scale i, undecimated wavelet coefficients can be written as

$$w_i = \{Q_\perp(TR_0(c_{i-1}))\} \ \overrightarrow{\cup} \ \{Q_\perp(TR_1(c_{i-1}))\}. \quad (34)$$

The expression (34) can be formulated according to the scale c_{i-2}

$$\begin{aligned} w_i = {} & Q_\perp TR_0\Big[\{P_\perp TR_0(c_{i-2})\} \ \overrightarrow{\cup} \ \{P_\perp TR_1(c_{i-2})\}\Big] \\ & \overrightarrow{\cup} \ Q_\perp TR_1\Big[\{P_\perp TR_0(c_{i-2})\} \ \overrightarrow{\cup} \ \{P_\perp TR_1(c_{i-2})\}\Big]. \end{aligned} \quad (35)$$

The two operators $Q_\perp$ and $P_\perp$ are distributive on the combination with an intertwining $\overrightarrow{\cup}$. Because of the downsampling, two successive shift operators and two projection operators can be resume with

$$Q_\perp\big[TR_b\big(P_\perp(TR_a[c_l])\big)\big] = Q_\perp P_\perp\big(TR_{a2+b}[c_l]\big).$$

Then (35) can be written as

$$\begin{aligned} w_i = {} & Q_\perp P_\perp TR_0[c_{i-2}] \ \overrightarrow{\cup} \ Q_\perp P_\perp TR_1[c_{i-2}] \\ & \overrightarrow{\cup} \ Q_\perp P_\perp TR_2[c_{i-2}] \ \overrightarrow{\cup} \ Q_\perp P_\perp TR_3[c_{i-2}] \\ = {} & \Big\{d_i^{0/i-2}\Big\} \ \overrightarrow{\cup} \ \Big\{d_i^{1/i-2}\Big\} \ \overrightarrow{\cup} \ \Big\{d_i^{2/i-2}\Big\} \ \overrightarrow{\cup} \ \Big\{d_i^{3/i-2}\Big\}. \end{aligned}$$

By recursivity, we obtain

$$w_i = \overrightarrow{\bigcup_{k=0\cdots 2^i-1}} Q_\perp(P_\perp)^{i-1}\big[TR_k(f)\big]. \quad (36)$$

Appendix II

If $\tilde{f}$ is a function obtained after inverse transformation of thresholded undecimated wavelet coefficients and $\tilde{f}_b$ corresponds to the inverse transform after denoising with the algorithm of Donoho–Johnstone on the shift function $TR_b(f)$, then

$$\tilde{f} = \frac{1}{2^L}\Big[\tilde{f}_0 + \tilde{f}_1 + \cdots + \tilde{f}_b + \cdots + \tilde{f}_{2^L-1}\Big].$$

Proof: Thereafter, to simplify equations, we will write the thresholding $T_{\lambda_i}(w_i)$ by Tw_i and $T_{\lambda_i}(d_i^{k/l})$ by $Td_i^{k/l}$.

$\tilde{f}$, the function obtained after invert transformation of wavelets coefficients thresholded is such that

$$\begin{aligned} \tilde{f} = {} & Q_u^{-1}Tw_1 + P_u^{-1}c_1 \\ = {} & Q_u^{-1}T\Big[d_1^{0/0} \ \overrightarrow{\cup} \ d_1^{1/0}\Big] + P_u^{-1}\Big[s_1^{0/0} \ \overrightarrow{\cup} \ s_1^{1/0}\Big] \\ = {} & Q_u^{-1}\Big[Td_1^{0/0} \ \overrightarrow{\cup} \ Td_1^{1/0}\Big] + P_u^{-1}\Big[s_1^{0/0} \ \overrightarrow{\cup} \ s_1^{1/0}\Big]. \end{aligned} \quad (37)$$

The opposite operator in the undecimated case is

$$\begin{aligned} Q_u^{-1}\Big[d_1^{0/0} \ \overrightarrow{\cup} \ d_1^{1/0}\Big] &= \tfrac{1}{2}\Big[Q_\perp^{-1}d_1^{0/0} + Q_\perp^{-1}d_1^{1/0}\Big] \\ P_u^{-1}\Big[s_1^{0/0} \ \overrightarrow{\cup} \ s_1^{1/0}\Big] &= \tfrac{1}{2}\Big[P_\perp^{-1}s_1^{0/0} + P_\perp^{-1}s_1^{1/0}\Big]. \end{aligned} \quad (38)$$

The (37) can therefore be written

$$\tilde{f} = \tfrac{1}{2}\left[Q_{\perp}^{-1}\left(Td_1^{0/0}\right) + Q_{\perp}^{-1}\left(hd_1^{1/0}\right)\right] + \tfrac{1}{2}\left[P_{\perp}^{-1}s_1^{0/0} + P_{\perp}^{-1}s_1^{1/0}\right].$$

The calculation can continue with $s_1^{0/0}$ (i.e $s_1^{1/0}$) by

$$\begin{aligned} s_1^{0/0} &= Q_u^{-1}T\left[d_2^{0/0} \ \overrightarrow{\cup} \ d_2^{1/0}\right] + P_u^{-1}\left[s_2^{0/0} \ \overrightarrow{\cup} \ s_2^{1/0}\right] \\ &= \tfrac{1}{2}\left[Q_{\perp}^{-1}\left(Td_2^{0/0}\right) + Q_{\perp}^{-1}\left(Td_2^{1/0}\right)\right] \\ &\quad + \tfrac{1}{2}\left[P_{\perp}^{-1}s_2^{0/0} + P_{\perp}^{-1}s_2^{1/0}\right]. \end{aligned}$$

By repeating the calculation, we finally have

$$\begin{aligned} \tilde{f} &= \frac{1}{2}\left[Q_{\perp}^{-1}\left(Td_1^{0/0}\right) + Q_{\perp}^{-1}\left(Td_1^{1/0}\right)\right] \\ &= \sum_{i=1}^{L}\left(\frac{1}{2^i}P_{\perp}^{-(i-1)}\left[\sum_{k=0}^{2^i-1}Q_{\perp}^{-1}\left(Td_i^{k/0}\right)\right]\right) \\ &\quad + \frac{1}{2^L}\sum_{k=0}^{2^L-1}P_{\perp}^{-L}s_L^{k/0}. \end{aligned} \tag{39}$$

By developing and making appropriate reassemblies, (39) can be rewritten as

$$\begin{aligned} \tilde{f} = \frac{1}{2^L}\Bigg[&\left[\sum_{i=1}^{L}\left(P_{\perp}^{-(i-1)}Q_{\perp}^{-1}\left(Td_i^{0/0}\right)\right)|! + |!P_{\perp}^{-L}s_L^{0/0}\right]\cdots \\ &+ \left[\sum_{i=1}^{L}\left(P_{\perp}^{-(i-1)}Q_{\perp}^{-1}\left(Td_i^{k/0}\right)\right)|! + |!P_{\perp}^{-L}s_L^{k/0}\right]\cdots \\ &+ \left[\sum_{i=1}^{L}\left(P_{\perp}^{-(i-1)}Q_{\perp}^{-1}\left(Td_i^{2^L/0}\right)\right)|! + |!P_{\perp}^{-L}s_L^{2^L/0}\right]\Bigg]. \end{aligned} \tag{40}$$

The expression

$$\tilde{f}_b = \left[\sum_{i=1}^{L}\left(P_{\perp}^{-(i-1)}Q_{\perp}^{-1}\left(Td_i^{b/0}\right)\right) + P_{\perp}^{-L}s_L^{b/0}\right]$$

corresponds to the denoising result with the algorithm of Donoho–Johnstone on the shift function $TR_b(f)$. Therefore, the function $\tilde{f}$, defined by (40), is equal to

$$\tilde{f} = \frac{1}{2^L}\left[\tilde{f}_0 + \tilde{f}_1 + \cdots + \tilde{f}_b + \cdots + \tilde{f}_{2^L-1}\right]. \tag{41}$$

REFERENCES

[1] C. Marque, J. Duchene, S. Leclercq, G. Panczer, and J. Chaumont, "Uterine EHG processing for obstetrical monitoring," *IEEE Trans. Biomed. Eng.*, vol. BME-33, pp. 1182–1187, Dec. 1986.

[2] J. Gondry, C. Marque, J. Duchene, and D. Cabrol, "Electrohysterography during pregnancy: Preliminary report," *Biomed. Instrum., Technol.*, vol. 27, pp. 318–324, 1993.

[3] C. Steer and G. Hertsch, "Electrical activity of human uterus in labor: The electrohysterograph," *Amer. J. Obstet. Gynecol.*, vol. 59, pp. 25–40, 1950.

[4] C. Sureau, "Etude de l'activité électrique de l'utérus au cours du travail," *Gynecol. Obstet.*, vol. 55, no. 2, pp. 153–173, 1956.

[5] G. Wolfs and M. Van Leeuwen, "Electromyographic observations on the human uterus during labour," *Acta. Obstet. Gynec. Scand.*, vol. 90, pp. 1–61, 1979.

[6] J. Planes, J. Morucci, H. Grandjean, and R. Favretto, "External recording and processing of fast electrical activity of the uterus in human parturition," *Med. Biol. Eng., Comput.*, vol. 22, pp. 585–591, 1984.

[7] H. Leman, C. Marque, and J. Gondry, "Use of the EHG signal for the early detection of preterm deliveries," to be Submitted.

[8] M. Holschneider, R. Kronland-Martinet, J. Morlet, and P. Tchamitchian, "A real-time algorithm for signal analysis with the help of the wavelet transform," in *Wavelet, Time-Frequency Methods and Phase Space*, J. Combes, A. Grossmann, and P. Tchamitchian, Eds. Berlin, Germany: Springer-Verlag, 1989, pp. 289–297.

[9] A. Bijaoui, J. Starck, and F. Murtagh, "Restauration des images multi-echelles par l'algorithme a trous," *Traitement du Signal*, vol. 11, pp. 232–243, 1994.

[10] J. Starck, F. Murtagh, and A. Bijaoui, "Multiresolution support applied to image filtering and restoration," *Comput. Vision, Graphics, Image Processing*, vol. 57, no. 5, pp. 420–431, 1995.

[11] C. Marque and J. Duchene, "Human abdominal EHG processing for uterine contraction monitoring," in *Applied Biosensor*, D. Wise and G. Webb, Eds. London, U.K.: Butterworths, 1989, pp. 187–226.

[12] S. Mansour, "Etude de l'électromyogramme utérin: Caractérization, propagation, modélization des transferts," Ph.D. dissertation, Univ. Technol. of Compiégne, Compiegne, France, 1993.

[13] S. Mallat, "A theory for multiresolution signal decomposition: The wavelet transform," *IEEE Trans. Pattern Anal. Machine Intell.*, vol. 11, pp. 674–693, 1989.

[14] P. Burt and E. Adelson, "The Laplacien pyramid as a compact image code," *IEEE Trans. Commun.*, vol. COMM-31, pp. 482–550, 1983.

[15] A. Cohen, *Ondelettes et Traitement Numérique du Signal*. Paris, France: Masson, 1992.

[16] A. Cohen and J. Kovacevic, "Wavelet: The mathematical background," *Proc. IEEE (Special Issue on Wavelets)*, vol. 84, pp. 514–522, Apr. 1996.

[17] M. Shensa, "Wedding the à trous and Mallat algorithms," *IEEE Trans. Signal Processing*, vol. 40, no. 10, pp. 2464–2482, 1992.

[18] D. Donoho, "Wavelet shrinkage and w.v.d.: A 10-minute tour," Stanford Univ., Stanford, CA, Tech. Rep., 1992.

[19] G. Nason, "Wavelet shrinkage using cross-validation," *J. Roy. Statist. Soc. B*, vol. 58, pp. 463–479, 1996.

[20] D. Donoho, "De-noising by soft-thresholding," *IEEE Trans. Inform. Theory*, vol. 41, no. 3, pp. 613–627, 1995.

[21] I. Johnstone and B. Silverman, "Wavelet threshold estimators for data with correlated noise," *J. Roy. Statist. Soc.*, 1996.

[22] R. Coifman and S. Donoho, "Translation-invariant de-noising," in *Wavelets and Statistics*, A. Antoniadis and G. Oppenheim, Eds., *Lecture Notes in Statistics*, vol. 103. New York: Springer-Verlag, 1995, pp. 125–150.

[23] I. Daubechies, *Ten Lectures on Wavelets*. Philadelphia, PA: SIAM, 1992.

[24] P. Carré, D. Boichu, P. Simard, and C. Fernandez, "Débruitage par transformée en ondelettes nondécimée: Extension aux acquisitions multiples," submitted for publication.

[25] L. Qiu, H. Yang, and S. Koh, "Fundamental frequency determination based on instantaneous frequency estimation," *Signal Processing*, vol. 44, pp. 233–241, 1995.

[26] D. Devedeux, "Evaluation quantitative de certaines caractéristiques de distributions temps-fréquence: Application á l'EMG *utérin*," Ph.D. dissertation, Univ. of Technology of Compiégne, Compiegne, France, 1995.

Philippe Carré was born in France on January 7, 1973. He received the Engineer degree in computer engineering from Compiegne University of Technology, Compiegne, France, in 1995. He is currently working in the CNRS Image and Signal Ircom-SIC laboratory towards the Ph.D. degree in Poitiers University at the Futuroscope of Poitiers. His interests include signal and image processing, wavelets, Time-Frequency and multiscale edge decomposition.

Hélène Leman was born in France on May 10, 1973. She received the Engineer degree in biomedical engineering from Compiegne University of Technology, Compiegne, France, in 1996 and is currently working towards the Ph.D. degree in the Department of Biomedical Engineering at the same university. Her interests include nonstationary signal processing and discrete and continuous wavelet analysis.

Christine Fernandez was born in France on November 26, 1962. She received the Computer Engineer degree from the Compiegne University of Technology, Compiegne, France, in 1986 and the Ph.D. degree in computer science from the same university in December 1989.

She is currently a Professor in Signal and Image Processing at the University of Poitiers, in the CNRS laboratory SIC at the Futuroscope of Poitiers.

Catherine Marque was born in France on January 15, 1958. She received the Engineer degree from the Ecole Nationale Superieure des Arts et Metiers in 1980 and the Ph.D. degree from Compiegne University, Compiegne, France, in 1987.

She is currently an Associate Professor at Compiegne University in the Biological Engineering Department, where she manages the biomedical engineering formation. Her interests include signal processing and instrumentation applied to the biomedical field.